The Efficiency of Ecballium Elaterium Extract as Green Inhibitor for Carbon Steel Corrosion in Sulfuric Acid

G.E. Badr*, Amera Ali, A.S. Fouda

Department of Chemistry, Faculty of Science, El-Mansoura University, El-Mansoura-35516, Egypt
*E-mail: badrgamila@mans.edu.eg

The inhibiting influence of Ecballium elaterium extract on the dissolution of carbon steel in 0.5 M sulfuric acid was studied using different methods, including mass loss, electrochemical impedance spectroscopy, potentiodynamic polarization and electrochemical frequency modulation. The tested compound was a mixed-type inhibitor, conforming to Temkin's adsorption isotherm model and included competitive chemisorption and physisorption mechanisms. The effectiveness of the inhibitor increased with increasing temperature and concentration. The morphology of carbon steel surface and the change on the surface after the inhibition process were studied by Atomic Force Microscopy and Fourier Transforms Infrared Spectroscopy techniques. Some quantum chemical parameters were calculated using the density functional theory to explain which types of phytochemical compounds found in the Ecballium elaterium extract had high efficiency towards the corrosion inhibition of carbon steel in acidic media. All test methods gave corresponding results.

Keywords: Ecballium extract, Corrosion inhibition, Carbon steel, Sulfuric acid, Temkin isotherm.

1. INTRODUCTION

One of the greatest and most interesting subjects for researchers and for the manufacturing industry in the latest years is the corrosion of metals and alloys. Metals are very important in our lives and have different metallic properties and they also have many uses. In general, all metals are unstable thermodynamically, and therefore, they react with the environment to return to their stable state, and this is one of the reasons causing erosion. Corrosion is a damaging process that weakens the metal and affects its intrinsic physical and chemical properties, leading to a critical problem in most manufacturing processes. This problem is a repeated one, and it is often difficult to be completely solved, and one of the best solutions to tackle this problem is to apply inhibition. Corrosion processes progress quicker after the distraction of the protective layer, leading to a change in the composition and properties of both the metal surface and the environment. Carbon steel is a metal of choice owing to its characteristic features,

as well as the widespread application features in many manufacturing processes. Acid solutions such as hydrochloric and sulfuric acids are usually used in industrial acid cleaning, acid descaling, oil well acidizing and acid pickling [1], and this process results in the dissolution of iron in acid solutions. The use of organic compounds as corrosion inhibitors, has shown to be the most efficient and practical way of preventing metal corrosion. The corrosion inhibitors of organic compounds differ from inorganic inhibitors, in that the organic compounds contain elements such as N, O, P and S in their heterocyclic rings, as well as macrocyclic compounds such as polymers [2]. The poisonousness of synthetic corrosion inhibitors has restricted their uses due to the accompanying environmental risks, and therefore, scientists turned aside from it and started to look for green inhibitors [3,4]. The vast majority of plant extracts from the world are reported to have excellent anticorrosive properties and are considered as possible inhibitors to eliminate corrosion in many industrial solutions [5]. Therefore, the use of natural products such as plant extracts as corrosion inhibitors for metals and alloys [6,7] has recently been encouraged because they are eco-friendly, low cost, renewable and readily available. The existence of all these features in the Ecballium elaterium extract caused the researchers of this paper to do the current research to examine its inhibition influence on the corrosion of carbon steel in 0.5 M H_2SO_4 using chemical and electrochemical methods. Additionally, Atomic Force Microscopy was used to investigate the surface morphology of the metal. Moreover, Fourier Transforms Infrared Spectroscopy was utilized to characterize the film adsorbed on the carbon steel surface. Finally, the inhibition performance and mechanism were discussed in this study based on the results obtained from all conducted experiments.
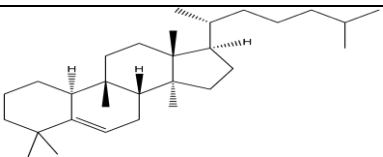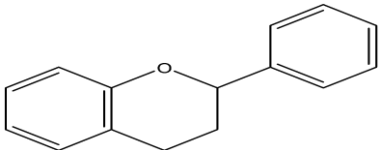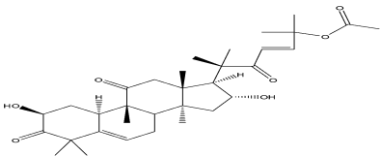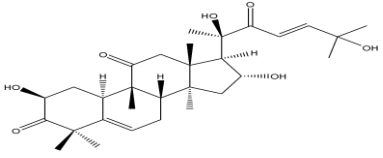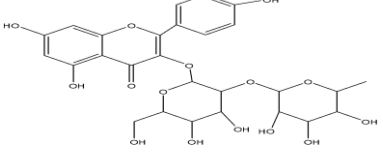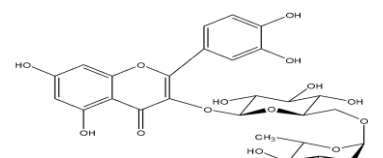
2. EXPERIMENTAL

2.1. Materials preparation

Carbon steel (CS) specimens composed of (wt. %) (0.610 C, 0.754 Mn, 0.013 P, 0.254 Si and balance Fe) were used for all research experiments. Analytical grade H_2SO_4 (98 wt. %) was utilized to prepare the aggressive medium of 0.5 M H_2SO_4 by dilution with bidistilled water.

The Ecballium elaterium extract was prepared from the fruits of the Ecballium elaterium plant growing in the wild plants in Sinai, Egypt. It was washed gently with bidistilled water, dried for 7 days in a ventilated room at 40°C, then ground to a fine powder using a mill. The extract was obtained by maceration of 250 g of powdered material with 500 ml methanol for 3 days at room temperature. Extract solutions were filtered by filter paper, and the solvent was collected and concentrated using a rotary evaporator at 35-55°C to obtain the solid extract. A series of concentrations ranging from 50 to 300 mg/L from the extract employed in this research was prepared by dilution with bidistilled water using a stock solution of 1000 mg/L. The chemical structure of some main phytochemical compounds isolated from the Ecballium elaterium extract was shown in Table 1 below [8].

Int. J. Electrochem. Sci., 16 **(2021)** Article ID: 210832

3

Table 1. Some phytochemical compounds isolated from the Ecballium elaterium extract.

S. no.	Name	Structure
I	Cucurbitane	
II	Flavonoids	
III	Cuc P	
IV	Cuc D	
V	Kaempferol-3-o-rutinoside	
VI	Rutin	

2.2. Mass loss (ML) tests

The carbon steel (CS) samples were cutaway to 2.0 cm x 2.0 cm x 0.2 cm for tests, abraded with several emery papers with a grade ranging from 400 to 1200, cleaned by bidistilled water, degreased with acetone, and dried carefully by filter papers. The samples were submerged for three hours in 100 ml of 0.5 M H_2SO_4 with and without concentrations (50, 100, 150, 200, 250, and 300 mg/L) of Ecballium elaterium extract at a temperature of 298, 303, 308, 313 and 318 K respectively. The weight of CS specimens was calculated before and after the immersion in the test solution. The total time of the immersion in the test solution was three hours and the specimens were taken from the test solution every 30 min to be weighed. All experiments were repeated three times for reproducibility and the mean value of the weight loss was reported and recorded to the nearest 0.0001g. The degree of surface coverage (θ) and the inhibition efficacy (*%IE*) of CS were calculated using the following two equations respectively[9].

$$\theta = \frac{W_{free} - W_{inh}}{W_{free}} \tag{1}$$

$$\%IE = \theta \text{ x } 100 = \frac{W_{free} - W_{inh}}{W_{free}} x \text{ } 100 \qquad (2)$$

where $W_{free} \text{ } and \text{ } W_{inh}$ are the ML of CS in blank and after adding the Ecballium extract, respectively.

2.3. Electrochemical Tests

All electrochemical tests were administered using the Gamry instrument PCI4/300 (Potentiostat/Galvanostat/Zra) analyzer which includes DC105, EIS300 and EFM140 for potentiodynamic polarization (PDP), electrochemical impedance spectroscopy (EIS) and electrochemical frequency modulation (EFM) measurements, respectively. The data was collected using a computer. The plotting, graphing and fitting of the data were conducted using the Echem Analyst 5.5 software. All tests were run in a classical tri-electrode glass cell, in which the working electrode (WE) was a CS specimen embedded in epoxy resin, leaving 1 cm^2 as a working surface area, while the counter electrode (CE) was a platinum sheet and the reference electrode was a saturated calomel electrode (SCE). The working electrode was treated as in ML tests then immersed for 30 minutes into the test solution at 25°C using water thermostat until the constant open-circuit potential (OCP) was reached. PDP curves were obtained by changing the electrode potential from +500 to -500 mV at OCP with a scan rate of 0.5 mV/s to give more data about the processes taking place at the CS/solution interface. The *%IE* and θ values were calculated through the following equation [10]:

$$\% \text{ } IE = \frac{i^{\circ}_{corr} - i_{corr}}{i^{\circ}_{corr}} x \text{ } 100 = \text{ } \theta \text{ } x \text{ } 100 \qquad (3)$$

where i°_{corr} and i_{corr} were the corrosion current densities in blank and after adding the Ecballium elaterium extract, successively. The EIS experiments were performed at a frequency ranging from 100 kHz to 0.5 Hz using an AC signal with 10 mV amplitude perturbation at the corrosion potential. The *% IE* and (θ) of the Ecballium extract were calculated using the following equation [11]:

$$\% \text{ } IE = \frac{R^{\circ}_{ct} - R_{ct}}{R_{ct}} x \text{ } 100 \qquad (4)$$

where R°_{ct} and R_{ct} were the charge transfer resistances for the blank and extract containing media respectively. The EFM was achieved using frequencies at 2 and 5 Hz with 1 Hz base frequency and by using the 1-second repeated waveform. The lower frequency must be at least half of the higher one. The *% IE* was calculated using the equation (3). The causality factors (CF) were the main advantage of EFM and used as an inner check for the rationality of the experiments.

2.4. Atomic Force Microscopy (AFM) analysis

The Atomic Force Microscopy (AFM) analysis was performed in utilizing mode using Nanosurf, Flex AFM 3 instrument with the scan area of 10 x10 mm^2, and a 1 Hz scan rate with data points of 256 x256. The AFM tests were run in contact mode using a Nano conductive silicon probe and Nanosurf C3000 software (Version 3.5.0.31). The 2D and 3D images (the extent of corrosion damage) for pure CS, in terms of surface roughness were acquired from the AFM analysis, after being dripped for 24 hours in the blank with and without Ecballium extract.

2.5. Fourier Transforms Infrared Spectroscopy (FTIR) analysis

Nicolet iS10 FT-IR spectrometer (USA) was used to analyze the pure Ecballium extract and the CS samples within 24 hours after being dripped in a test solution with Ecballium extract to get FTIR spectra.

2.6. Computational studies

The quantum chemical calculations for the phytochemical isolated compounds of Ecballium extract were performed using the DFT approach. The optimization of the molecular structure was performed using DMol^3 module of materials studio, version 7. The Becke's one parameter with generalized gradient approximation and a basic set of double number polarization plus were also performed. The COSMO model was used to treat the effect of water as a solvent during the optimization evolution.

3. RESULTS AND DISCUSSION

3.1. ML tests

The ML-time plots for the dissolution of CS in 0.5 M H_2SO_4 with and without different concentrations of Ecballium extract at 298 K were given in Fig. 1. It elucidated that the ML of CS was decreased with increasing Ecballium extract concentrations. The calculated *% IE* of Ecballium extract at different concentrations increased with increasing concentration and reached to 83.4 % for 300 mg/L. This could have been ascribed to the adsorption of the extract molecules on the CS surface which created a barrier, isolated the surface of CS from the acidic solution and decreased the CS dissolution.
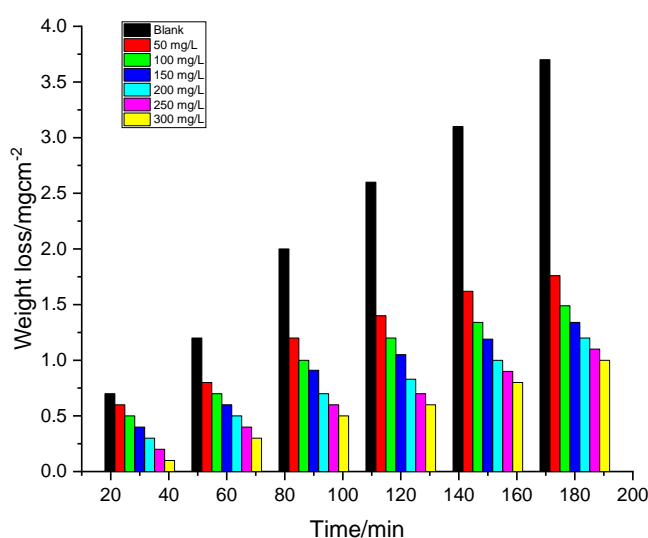

Figure 1. ML-time curve for the dissolution of CS in 0.5M H_2SO_4 as blank and after adding various concentrations of Ecballium extract to the test solution at 25°C.

3.2. Electrochemical Measurements

3.2.1. PDP measurements

Tafel curves of CS in 0.5 M H_2SO_4 as blank and after adding various concentrations of Ecballium extract at 25°C were presented in Fig. 2. Some parameters like corrosion potential (E_{corr}), corrosion current density (i_{corr}), cathodic and anodic Tafel slopes (β_c and β_a), corrosion rate (k_{corr}), θ and *% IE* were evaluated as per the corresponding curves and they were listed in Table 2. In this sense, Table 2 exhibited that there was a regular displacement in the corrosion potential (E_{corr}) values because of the decrease of i_{corr}. In the same manner, the values of β_c and β_a decreased when the extract was added to the corrosive media, providing confirmatory evidence in support of the presence of an extract that acts as a mixed inhibitor according to Li and others [12]. Furthermore, Fig. 2 showed typical PDP curves for the CS specimen in 0.5 M sulfuric acid solution with and without various doses of the extract. The plots revealed that the metal undertook the active dissolution with no distinctive transition to passivation within the studied potential range. The adding of the extract to the corrosive medium affected both the anodic dissolution and the cathodic hydrogen evolution curves, while the corrosion potential, E_{corr}, was only slightly shifted. This implied that the extract acted as a mixed type inhibitor when the absolute difference in E_{corr} did not exceed $\pm 85\ mV$ [13]. Along with the same lines, the addition of various concentrations of Ecballium extract to the CS in 0.5 M H_2SO_4 made a slight shift in E_{corr} values, about $(30\ mV)$ in relation to the blank. Adding to this, the values of (β_a and β_c) did not change remarkably, disclosing that both the dissolution process of CS and the liberated hydrogen mechanism were not affected. Moreover, a decrease of (i_{corr}) was observed with an increase in the concentration of Ecballium Extract. This indicated the ability of extract molecules to enhance and block more active sites as they were necessary for the corrosion process, for lowering the k_{corr} values, for retarding both anodic and cathodic reactions and for increasing the *% IE*.
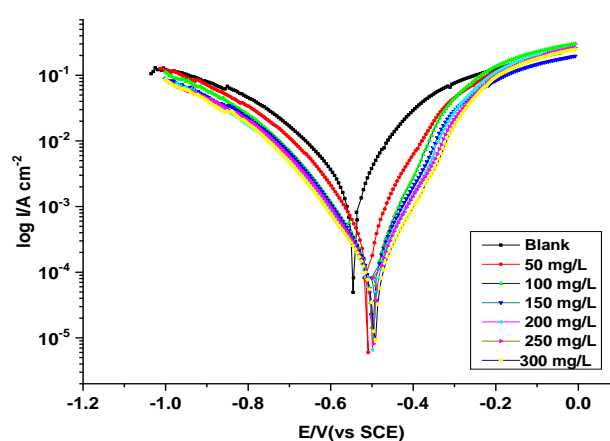

Figure 2. PDP curves of CS in 0.5 M H_2SO_4 as blank and with different concentrations of Ecballium extract at 25°C.

Table 2. PDP parameters and corresponding %IE for CS 0.5 M H$_2$SO$_4$ as blank and with various concentrations of Ecballium extract.

Conc, (mg/L)	i_{corr}, (μA cm^{-2})	$-E_{corr}$, (V vs SCE)	β_c, (Vdec^{-1})	β_a, (Vdec^{-1})	k_{corr}, (mpy)	Θ	IE%
Blank	584±0.003	0.541±0.020	0.234±0.031	0.072±0.003	266.8±0.2	--	--
50	164±0.002	0.529±0.017	0.209±0.028	0.069±0.003	75.1±0.33	0.719	71.9
100	115±0.003	0.527±0.026	0.187±0.019	0.068±0.004	28.5±0.23	0.803	80.3
150	111±0.003	0.523±0.031	0.200±0.025	0.065±0.002	27.5±0.19	0.809	80.9
200	62±0.002	0.521±0.029	0.189±0.027	0.061±0.004	52.6±0.27	0.893	89.3
250	60±0.003	0.516±0.023	0.200±0.026	0.059±0.003	50.9±0.12	0.897	89.7
300	44±0.002	0.512±0.030	0.183±0.012	0.044±0.001	20.1±0.34	0.925	92.5

3.2.2. EIS measurements

Figures 3 and 4 below displayed the Nyquist and Bode plots for the dissolution of CS in the blank and with various concentrations of Ecballium extract after the immersion for 30 min. respectively. The Nyquist plots generally comprised of only one depressed capacitive semicircle in the high frequency region which correspond to a one time constant in the Bode plots indicated that the dissolution of the CS electrode in the test solutions was controlled by the charge transfer process. The similar features of both Nyquist and Bode plots obtained with and without Ecballium extract affirmed that the mechanism of corrosion did not change after the compound was added to the corrosive media [10]. The depressed semicircles with a large capacitive loop might be considered a sign of the inhomogeneity at the electrode surface, a predominating feature owing to the adsorption of extract molecules, corrosion products, or metal inhibitor complex on the solid electrode surface. Moreover, the diameters of Nyquist semicircles increased by increasing the extract concentration, indicating higher resistivity of CS to the dissolution when the Ecballium extract was added. The tangible increase in the impedance modulus by increasing the extract concentration led to progressive parallel lines, and the broadening of the phase angle of the Bode plot indicated that the surface of CS was used as a shield with a film of Ecballium extract molecules to protect the metal surface from any further dissolution in the corrosive media. The equivalent circuit shown in Fig. 5 was used to derive the electrochemical kinetics parameters of the corrosion reaction by fitting and simulating the impedance spectra. The impedance of a CPE (Z_{CPE}) was calculated using the equation (5) [14].
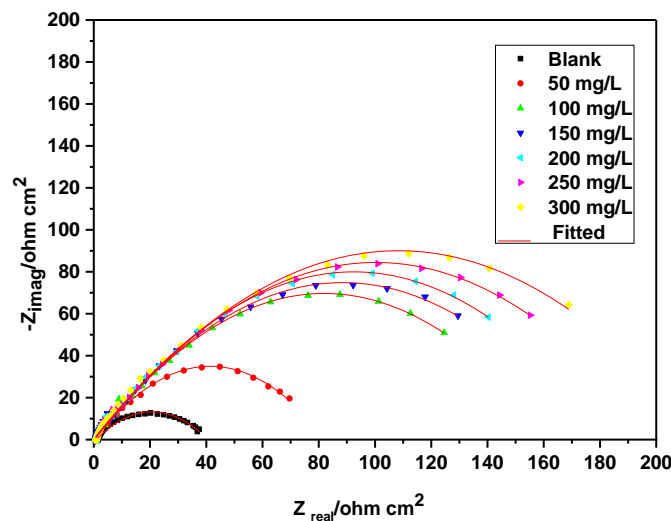
Figure 3. Nyquist plots of CS in 0.5 M H$_2$SO$_4$ before and after adding different concentrations of Ecballium extract.

$$Z_{CPE} = \frac{1}{Y_o \, (j\omega)^n} \tag{5}$$

where Y$_0$ stands for the CPE coefficient, j is the imaginary unit, n is the CPE exponent (phase shift), ($\omega = 2\pi \, F_{max}$) is the angular frequency in which the maximum AC frequency denotes by F_{max}. The double-layer capacitance (C$_{dl}$) was calculated as follows:

$$C_{dl} = Y_o \, (\omega_{max})^{n-1} \tag{6}$$

where ω_{max} stands for the angular frequency at the maximum impedance values obtained for the imaginary component. The EIS data listed in Table 3 below indicated an increase of charge transfer resistance (R$_{ct}$) values with increasing Ecballium extract concentration, and consequently, an increase in the inhibition efficiency (%IE). The heterogeneity of the surface could be studied via the evaluation of the 'n' parameter from the EIS data [15]. The values recorded in Table 3 below indicated that the lowest value of n (0.0809) was observed for the sample immersed in the H$_2$SO$_4$ solution only. This could have been accredited to the surface inhomogeneity from the metal surface damage and the ununiformed corrosion attack. The value of n approach to one by increasing the extract concentration denoted that the CS specimens exposed to the blank solution may have encountered no regular corrosion attack, leading to further inhomogeneity of the CS surface in comparison to those exposed to the inhibited solutions. The results from this observation may have been attributed to the adsorption of the extract molecules on the surface, a matter which resulted in more uniform erosion on the surface of CS. The polarization resistance (R$_s$) can measure the degree of difficulty in the charge transfer process through corrosion. The high values of Rs reflected a decline in the corrosion phenomenon. The values of Y_o were the magnitude of CPE which was considered a surface irregularity of the electrode that caused a greater depression in the Nyquist semicircle diagram and its values decreased with an increase in the extract concentration, indicating a more smoothing metal surface. Moreover, the decrease in the values of C$_{dl}$ by increasing the concentration of Ecballium extract molecules indicated a lower dielectric constant of the molecules which were adsorbed by substituting the water pre-adsorbed molecules on the interface of CS/solution

[16]. This construction of the adsorbed shielding film of the extract molecules inhibited the electrochemical corrosion of CS in an acidic medium.
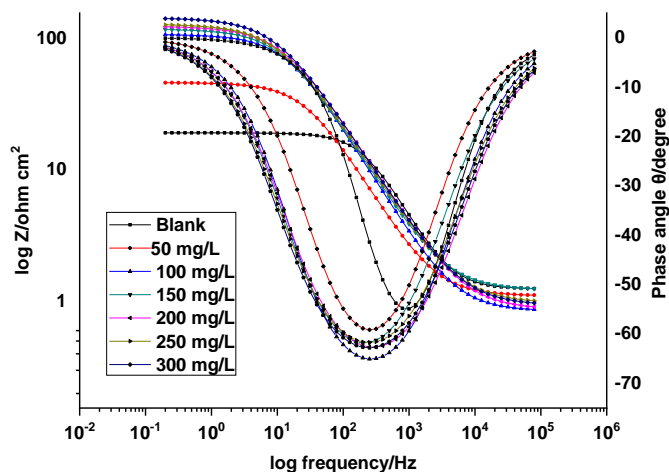

Figure 4. Bode diagrams for CS in 0.5M H_2SO_4 before and after adding various concentrations of Ecballium extract
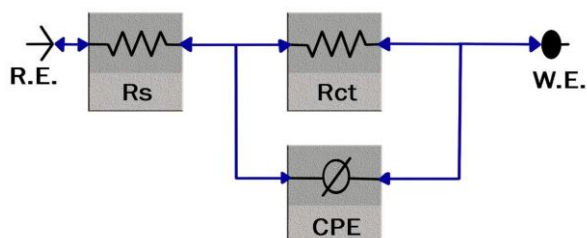

Figure 5. The electrochemical equivalent circuit used to fit the EIS spectra.

Table 3. The obtained EIS values for CS in 0.5M H_2SO_4 with and without various concentrations of Ecballium extract.

Conc. (mg/L)	Rs (Ω cm^2)	R_{ct} (Ω cm^2)	Y_0, ($\mu s^n cm^{-2}$)	n	θ	C_{dl} (μF cm^{-2})	*%IE*
Blank	2.9±0.04	26.0±0.04	471.6±0.003	0.809±0.020	----	214	----
50	5.1±0.07	79.2±0.02	471.4±0.004	0.816±0.004	0.672	211	67.2
100	5.8±0.06	115.2±0.03	312.6±0.003	0.824±0.003	0.774	181	77.4
150	7.2±0.06	127.9±0.04	302.4±0.006	0.830±0.005	0.797	146	79.7
200	7.8±0.08	148.6±0.06	369.1±0.005	0.845±0.004	0.825	141	82.5
250	8.4±0.07	174.6±0.05	331.4±0.003	0.850±0.002	0.851	133	85.1
300	8.7±0.06	203.6±0.08	329.8±0.002	0.854±0.006	0.872	105	87.2

It was then concluded that the decline in the capacity with the increase of Ecballium extract concentration can lead to an increase in the thickness of the double layer in accordance with the following Helmholtz's model [17]:

$$C_{dl} = \frac{\varepsilon \varepsilon_o A}{\delta} \qquad (7)$$

Where A is the electrode surface area, δ is the thickness of the protective layer, ε_o is the vacuum permittivity and ε is the dielectric constant of the medium.

The Bode plots were displayed in Fig. 4. The one peak observed in Bode plots for the extract exhibited the presence of a single time constant as mentioned in the Nyquist plot.

3.2.3. EFM measurements

The corrosion rate and corrosion kinetic parameters can instantaneously be measured using the EFM technique without prior knowledge of Tafel, and therefore, it is deemed a perfectly appropriate technique for monitoring corrosion. The intermodulation spectra of CS in the blank and after adding various concentrations of Ecballium extract in 0.5 M H_2SO_4 solutions at 298 K were shown in Fig. 6.

Table 4. The EFM parameters of CS erosion with and without various concentrations of Ecballium extract in 0.5 M H_2 SO_4 at 298 K

| Conc, mg/L	i_{corr}, $\mu A\ cm^{-2}$	β_a, mV dec^{-1}	β_c, mV dec^{-1}	k_{corr}, mpy	CF-2	CF-3	θ	IE %
Blank	52.0±0.002	77.2±0.004	110.4±0.035	0.123±0.023	1.86	2.63	----	----
50	25.7±0.003	61.7±0.002	195.3±0.031	0.117±0.031	1.96	2.91	0.507	50.7
100	15.8±0.003	57.9±0.003	148.4±0.028	0.072±0.038	1.92	2.99	0.696	69.6
150	14.9±0.004	59.6±0.002	159.9±0.031	0.068±0.028	1.95	2.98	0.713	71.3
200	12.4±0.002	59.7±0.002	136.4±0.011	0.057±0.029	1.93	2.72	0.761	76.1
250	10.4±0.002	63.5±0.002	153.9±0.026	0.047±0.019	1.92	2.92	0.801	80.1
300	10.2±0.002	56.5±0.004	135.8±0.022	0.047±0.017	1.88	3.00	0.804	80.4
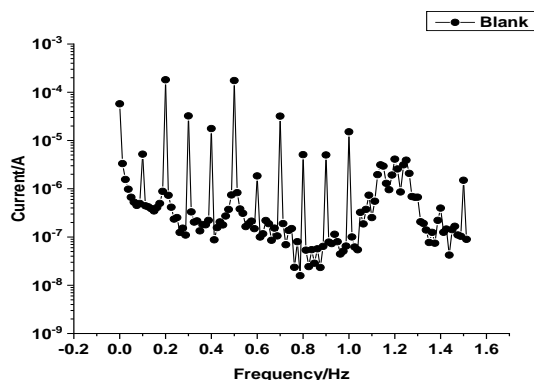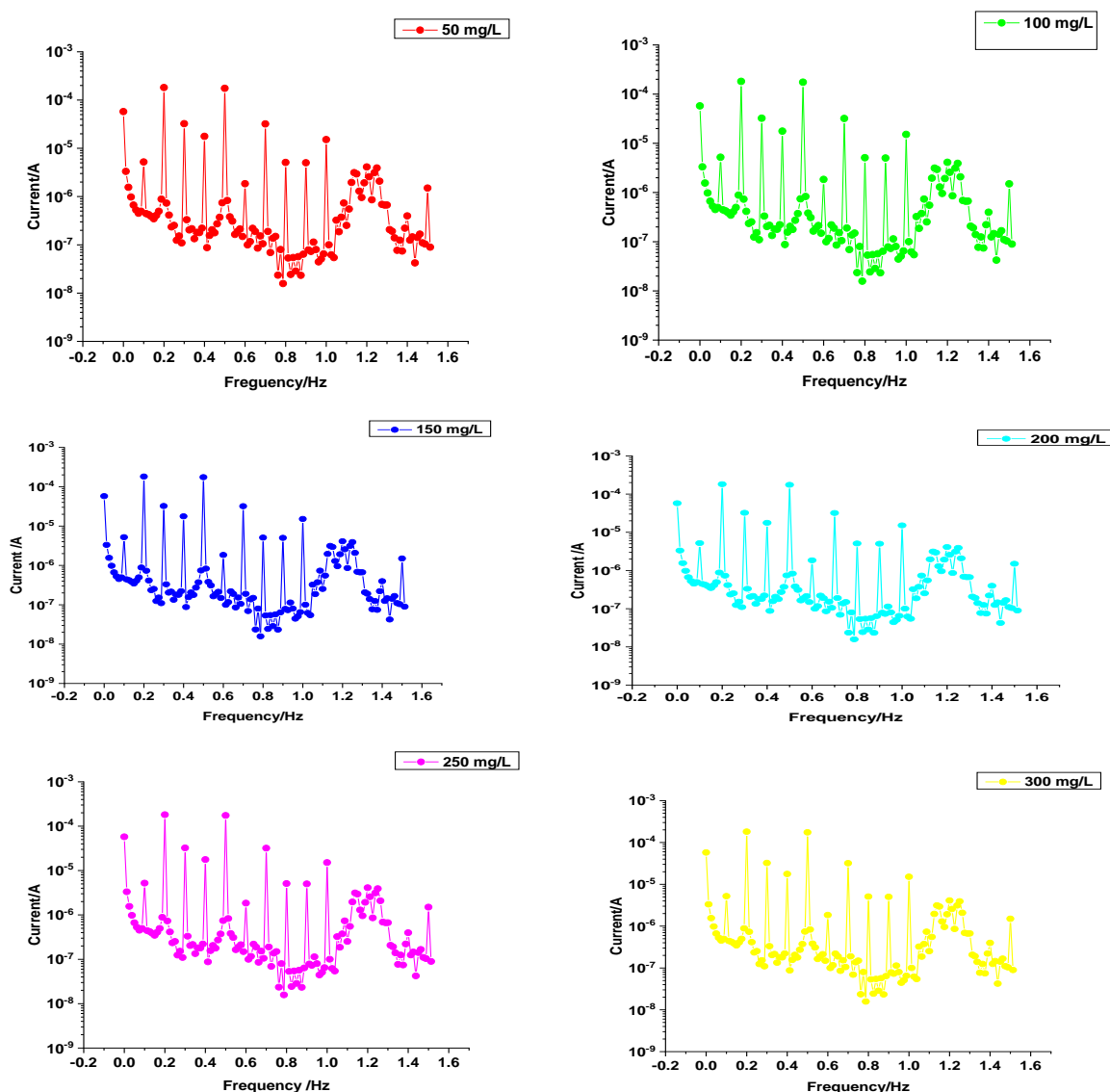
Figure 6. EFM spectra of CS in 0.5 M H_2SO_4 in the absence and presence of different concentrations of Ecballium extract.

The corrosion kinetic parameters obtained through the adoption of the EFM technique like i_{corr}, β_a, β_c, k_{corr}, causality factors (CF-2, CF-3), θ and %IE of various concentrations of Ecballium extract in 0.5 M H_2SO_4 at 25°C were recorded in Table 4 below. The results showed that the i_{corr} and k_{corr} values decreased while the %IE increased with increasing concentration of Ecballium extract. The values of the causality factors (CF-2 and CF-3) obtained were very close to the theoretical values (2 & 3) respectively in accordance with the EFM theory [18]. A smaller difference of causality factors than the standard values may have been put down to the frequency spectra resolution, to the perturbation amplitude or to the extract performance.

3.3. Adsorption Isotherms

The interaction between the inhibitor molecules and the metal surface can be done via Van der Waals force (physisorption) or by a chemical bond (chemisorption) or both. This interaction depends heavily on the nature of the electrolyte and the metal surface, the chemical structure of the extract, and the electrochemical potential at the metal/electrolyte border and it controls the propagation of adsorption and the efficiency of the extract [19]. The extract molecules started to adsorb competitively on the metal surface when the metal was immersed in an inhibited acid solution. Consequently, the equilibrium between the adsorbed and the non-adsorbed extract molecules in the bulk of the acid solution occurred and it could be defined through the adsorption isotherms. The adsorption of an organic adsorbate on a metal surface was considered as an alternative adsorption process between the organic molecule in the aqueous solution ($Org_{(sol)}$), and the water molecules adsorbed on the metallic surface ($H_2O_{(ads)}$) as follows [20]:

$$Org_{(sol)} + xH_2O_{(ads)} \leftrightarrow Org_{(ads)} + xH_2O_{(sol)} \tag{8}$$
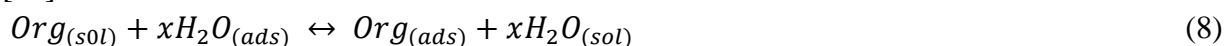
where x represents the number of replacement water molecules by one molecule of the organic adsorbate. The most appropriate isotherm was obtained by fitting the experimental data taken from the ML method with several adsorption isotherms, and the best fit was attained with Temkin adsorption isotherm as displayed in Fig. 7 below. The straight lines obtained from the plotting of θ against log C (eq. 9) at different temperatures of Ecballium extract in 0.5 M H_2SO_4 suggested that, the adsorption of extract on the CS surface obeyed the Temkin adsorption isotherm model.

$$\theta f = \log K_{ads} + \log C \tag{9}$$

where C is the extract concentration, θ is the surface coverage as determined by the ML method, K_{ads} is the adsorptive equilibrium constant, and *f is* the heterogeneous factor of the metal surface (*f = -2a), and* where *a* is the molecular interaction parameter that can have a positive value for the attraction or negative value for the repulsion between the adsorbed molecules. The attraction takes place if *f < 0* and the repulsion occurs if *f > 0*. The thermodynamic parameters for the adsorption process were recorded in Table 5 below. The K_{ads} values were computed from the intercept of the straight lines and the standard free energy of adsorption ΔG°_{ads} was obtained from the K_{ads} values through the following equation [10]:

$$\Delta G^{\circ}_{ads} = -RT \ln \ln (55.5 \, K_{ads}) \tag{10}$$

where the molar concentration of water in solution in M/L equals to 55.5 and the negative sign designates the spontaneity in the adsorption process. In previous studies, the ΔG°_{ads} values around -20 kJ mol^{-1} or less suggested physisorption, from -20 to -40 kJ mol^{-1} suggested mixed physisorption and chemisorption but around -40 kJ mol^{-1} or higher were chemisorption when connected with a coordinate type of metal bond by sharing or transferring a charge from the extract molecules to the metal surface [10]. The obtained values of ΔG°_{ads} of Ecballium extract exhibited that the extract molecules followed both physisorption and chemisorption at a temperature of (25-35ºC) but favored chemisorption at a temperature of (40 and 45ºC).
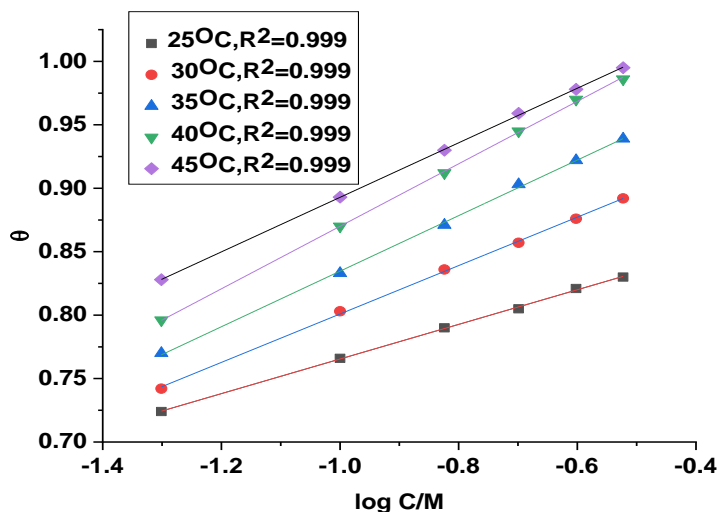
Figure 7. Temkin Adsorption isotherm curves for the adsorption of Ecballium extract on CS in 0.5 M H$_2$SO$_4$ at (25-45°C) from ML measurements

Also, the results proved that the attraction forces occurred between the adsorbed molecules in the adsorption layer when the heterogeneity factor *f* had a negative value, and the molecular interactions parameter had a positive value. The standard enthalpy ΔH°_{ads} and ΔS°_{ads} can be determined using the following equation:

$$\Delta G^\circ_{ads} = \Delta H^\circ_{ads} - T\Delta S^\circ_{ads} \tag{11}$$

The values of ΔH°_{ads} and ΔS°_{ads} were evaluated from the intercept and the slope of the straight line of the plot of ΔG°_{ads} versus *T*, respectively. The positive sign of ΔH°_{ads} values confirmed the endothermic of the adsorption process and the negative sign on ΔS°_{ads} values indicated that, during the adsorption process, the molecules of the Eclabium extract were organized on the CS surface and that the adsorption process favored the chemical adsorption, especially at higher temperatures.

Table 5. Adsorption Thermodynamic data of Ecballium extract on CS surface in 0.5M H$_2$SO$_4$ at (25-45°C).

Temp, °C	K_{ads}, 10^4 M^{-1}	- ΔG°_{ads}, kJ mol^{-1}	ΔH°_{ads} kJ mol^{-1}	-ΔS°_{ads} J mol^{-1} K^{-1}	-f	a
25	88.5	37.3		411.5	8.00	4.00
30	122.5	38.7		422.4	9.12	4.56
35	165.0	39.8	91.5	433.3	9.18	4.59
40	166.2	41.7		418.9	10.28	5.14
45	701.6	47.3		465.8	0.32	5.16

3.4. The influence of immersed Time and Temperature

The effect of immersed time on the inhibition efficiency of different concentrations of Ecballium extract on the dissolution of CS in 0.5M H$_2$SO$_4$ at (25-45°C) was examined by the ML method. The data included in Table 6 below presented the effect of immersed time on the %IE of CS in 0.5 M H$_2$SO$_4$ with

Int. J. Electrochem. Sci., 16 (**2021**) Article ID: 210832

14

300 mg/L Ecballium extract at various temperatures while the other concentrations were not shown. Also, the effect of temperature on %IE of CS after 180 min immersion in 0.5M H_2SO_4 with concentrations (50-300 mg/L) of Ecballium extract was examined and the results were exhibited in Table 7 below. The results revealed that the inhibition efficiency of the inhibitor increased with increasing both the immersion time and the temperature, implying the strong adsorption of the effective compounds in the Ecballium extract on the CS surface, and suggesting the creation of a barrier (protective film among the CS surface and the aggressive media) to prevent any further dissolution of the metal and to reinforce chemisorption at higher temperatures during the adsorption process.

Table 6. The effect of immersed time on the *%IE* of 300 mg/L Ecballium extract on the dissolution of CS in 0.5M H_2SO_4 at a temperature of (25-45°C) by the ML measurements.

Temp., K	25	30	35	40	45
Time, min			*%IE*		
30	57.9	79.4	84.1	90.1	93.8
60	75.3	81.6	85.9	92.8	95.6
90	75.9	82.8	89.1	93.3	95.9
120	82.3	88.5	92.1	95.7	97.2
180	83.4	89.3	93.4	96.2	97.5

Table 7. The effect of temperature on the (%IE) of CS after 180 min. of immersion in 0.5 M H_2SO_4 with concentrations (50-300 mg/L) of Ecballium extract by the ML measurements.

Conc., mg/L	50	100	150	200	250	300
Temp, K			%IE			
25	73.8	80.1	82	82.6	83	83.4
30	76	86.3	86.9	87.3	88.1	89.3
35	78.2	89	90.4	92	92.9	93.4
40	80.1	92.3	95.4	95.9	96	96.2
45	84.3	93	96.5	97	97.3	97.5

3.5. Thermodynamic Activation Parameters

The temperature studies provided information about the kinetics of the corrosion process. Therefore, the ML tests were carried out at temperatures from 25 to 45°C for the corrosion of CS in 0.5 M H_2SO_4 in the absence and presence of Ecballium extract (50 -300 mg/L). The activation parameters can be calculated using the following equations [21]:

$$log\ k_{corr} = \frac{E_a^*}{2.303RT} + log\ log\ \lambda \tag{12}$$

$$k_{corr} = \frac{RT}{Nh} exp\ exp\ \left(\frac{\Delta S_a^*}{R}\right) exp\ exp\ \left(\frac{-\Delta H_a^*}{RT}\right) \tag{13}$$

Where, k_{corr}, E_a^*, R, T, λ, N, h, ΔS_a^*, ΔH_a^* stand for corrosion rate, activation energy, the universal gas constant, the temperature in Kelvin, Arrhenius factor, Avogadro's number, Planck's constant, activation entropy and activation enthalpy respectively.
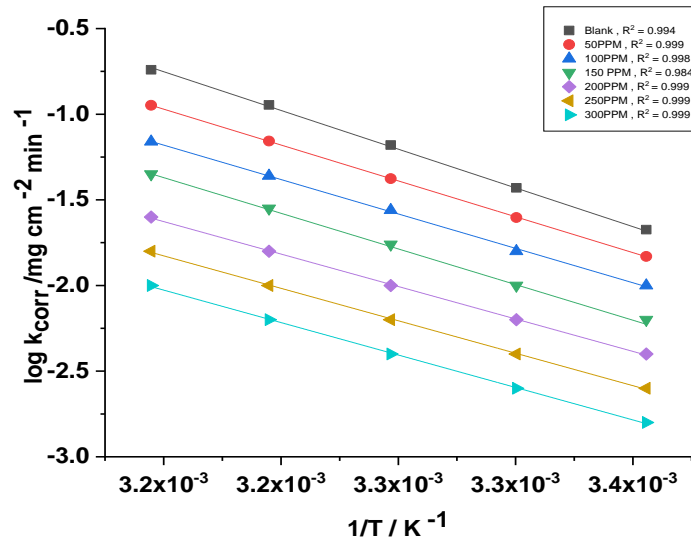

Figure 8. Arrhenius curves of CS corrosion rates $\left(log\ k_{corr}\ vs.\ \frac{1}{T}\right)$ in 0.5M $H_2\ SO_4$ with and without different concentrations of Ecballium extract after 120 minutes of immersion.
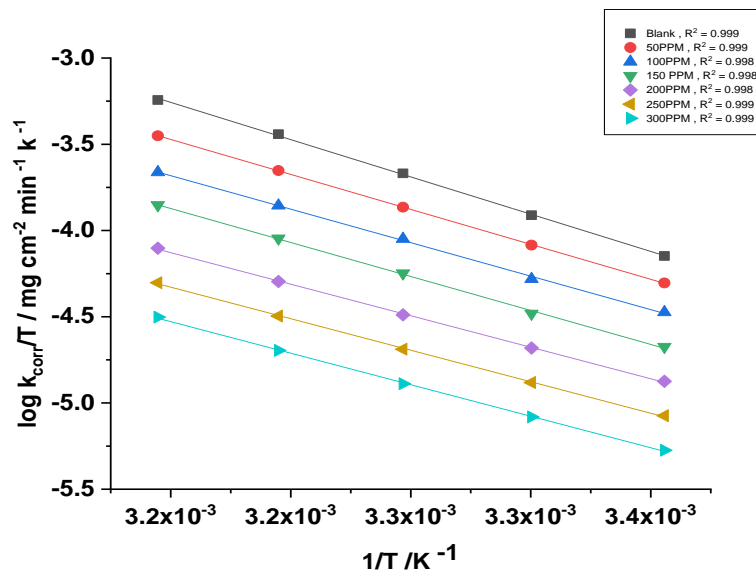

Figure 9. Transition-state curves of $\left(\frac{log\ k_{corr}}{T}\ vs.\ \frac{1}{T}\right)$ for CS in 0.5M H_2SO_4 in the absence and presence of different concentrations of Ecballium.

Table 8 below yielded the activation parameters evaluated from the slope and intercept of the straight lines of the graphs ($log\ k_{corr}\ vs.\ \frac{1}{T}$) and ($\frac{log\ k_{corr}}{T}\ vs.\ \frac{1}{T}$) as illustrated in Figures 8 and. 9

*Int. J. Electrochem. Sci.,* 16 (**2021**) Article ID: 210832

16

respectively. The results showed that the apparent activation energy value, E_a^*, for the blank solution, was 86.6 kJmol^{-1} and for different concentrations of Ecballium extract (50 – 300 mg/L) ranged from 81.6 to 28.3 kJmol^{-1} respectively, providing evidence that the activation energy decreases with the increase of inhibitor concentration. The decrease in the E_a^* values may have been the result of the chemical adsorption mechanism of the inhibitors on the CS surface by sharing or transferring the charge from the inhibitor to the CS surface, yielding a film and establishing a barrier between the CS surface and the aggressive media to prevent any further metal dissolution at higher temperatures. The positive sign of ΔH_a^* values denoted the endothermic nature of the corrosion process and the decrease in its values with increasing temperature affirmed the chemical adsorption mechanism [22]. As concluded from the results, the increase in the negative values of ΔS_a^* by increasing the extract concentration reflected that the rate-determining step for the activated complex represented an association rather than dissociation.

Table 8. Activation parameters for CS corrosion with and without different concentrations of Ecballium in 0.5 M H_2SO_4.

Conc., Mg/L	E_a^* kJ mol^{-1}	ΔH_a^* kJ mol^{-1}	$-\Delta S_a^*$ J mol^{-1} K^{-1}
Blank	86.6	80.5	6.8
50	81.6	75.4	26.8
100	58.8	56.2	131.3
150	31.7	29.2	192.2
200	26.8	24.3	213.1
250	28.6	26.0	206.4
300	28.3	25.7	204.4

3.6. AFM analysis

A topographical study of the CS surface was carried out by means of AFM from nano to micro-scale to investigate the effect of Ecballium extract on the production and proceed with the erosion process at the CS/solution interface [23]. The AFM images (2d and 3d) of CS with and without dipping in the test solution for 24 hours were presented in Fig. 10.
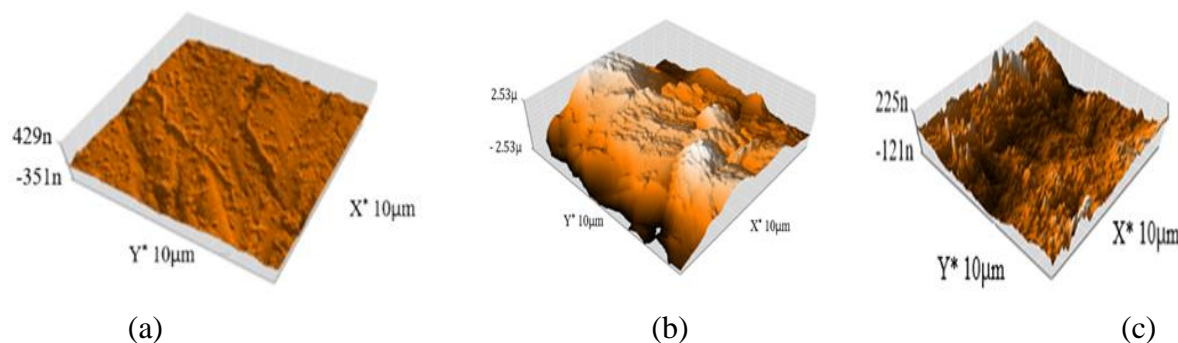
(a)   (b)   (c)
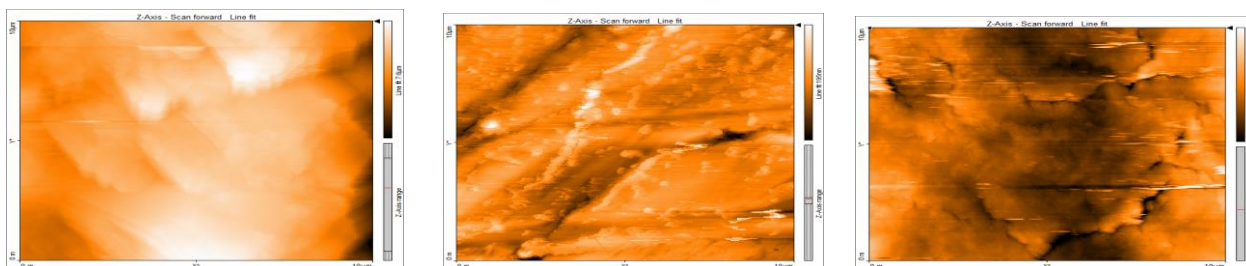
Figure 10. 2D and 3D-AFM micrographs of Pure CS (a), after being dripped in blank solution (b) and after being dripped in the blank with 300 mg/L Ecballium extract for 24 hours (c).

These images of the CS surface were significant in adding a large amount of measurable data concerning with the CS surface variations; the smooth surface of CS before being immersed in the test solution (a), the surface corroded in the presence of a blank solution (b) and the CS surface are smoother in the existence of 300 mg/L Ecballium extract (c). The roughness of the free CS was 17.47 nm. The maximum surface heterogeneity was noticed on the CS exposed to the blank solution, and the roughness increased to 994.01 nm. Similarly, the 2d and 3d images exhibited great valleys and peaks. In contrast, the destruction on the CS surface was very low with only slight spikes in the existence of 300 mg/L Ecballium extract in 0.5 M H_2SO_4. Also, the average surface roughness was lowered to 42.86 nm indicating better corrosion resistance. This indicated that the creation of a protective film through the adsorption of inhibitor molecules over the CS surface was developed in the existence of a high concentration of Ecballium extract**.**

3.7. FTIR analysis

FTIR spectroscopy is an analytical technique used to distinguish the functional groups existing in the extract, the type of interaction occurring among the extract molecules and CS surface and the nature of the chemical constituent adsorbed on the metal surface [24]. Fig. 11 (a) represented the FTIR spectra of pure Ecballium extract and (b) the protective film developed on the CS surface after being dripped for 24 hours in a test solution containing Ecballium extract. The spectra exhibited a characteristic absorption band of pure Ecballium extract at 3364, 2919, 2851, 1591, 1044, 1394 cm^{-1} agreeing to O-H, C-H, C-H, C=C, C-O (stretching) and C-H (bending) respectively, while the FTIR spectra of the protective film formed on the CS surface showed the same characteristic absorption bands with a small shift in the positions of the peaks and new weak peaks appeared at 1197, 1255, 3565 and 3645 cm^{-1} suggesting the occurrence of interaction between the CS surface and the extract molecules during the adsorption process and indicating a chemisorption mechanism.
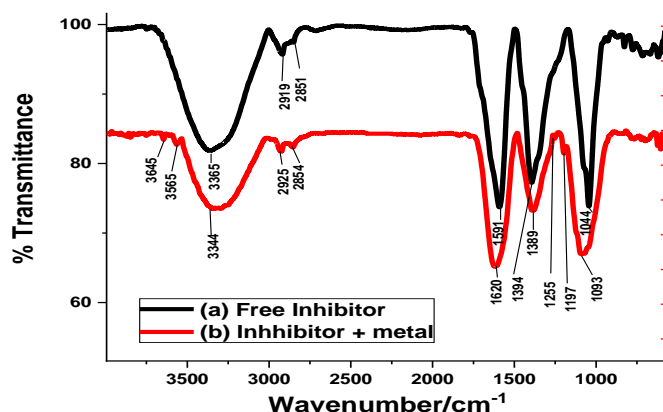
Figure 11. FTIR spectra (a) for pure Ecballium extract and (b) for CS surface after being dripped for 24 hours in a test solution containing Ecballium extract.

3.8 Quantum chemical calculations

Quantum chemical computation was used for the isolated phytochemical compounds (I to VI) of Ecballium extract to describe and compare the experimental results and to give an overview of the compounds that have more inhibition action on the corrosion 0f CS in acidic media. The frontier molecular HOMO and LUMO orbitals (the highest occupied molecular orbital and the lowest unoccupied molecular orbital) of chemical species were very important in defining its reactivity. Fig. 12 below displayed the optimized geometry, HOMO and LUMO for the isolated phytochemical compounds of Ecballium extract. Also, as shown in Figure 12, a planar array of all molecules, the HOMO, and the LUMO were not spread at all molecules but concentrated on a limited region of the molecules. The HOMO density distribution of the molecules concentrated on the left side of all molecules especially on the phenyl ring, the double bond in the ring, the heterocyclic oxygen and the substituents on the phenyl group, while the LUMO density distribution at the same side for compounds I, V and VI and on the right side of compounds II, III and IV, indicating the inductive electron-withdrawing effect in this direction. As recorded in Table 9, the obtained values of the frontier molecular orbital energies (E_{LUMO} and E_{HOMO}), as taken from the DMol^3 module of materials studio, were employed to calculate a set of important parameters using the following equations [25]:

$$\Delta E = (E_{LUMO} - E_{HOMO}) \tag{14}$$

$$\eta = -\frac{1}{2}(E_{HOMO} - E_{LUMO}) \tag{15}$$

$$\sigma = \frac{1}{\eta} \tag{16}$$

$$\chi = -\frac{1}{2}(E_{LUMO} + E_{HOMO}) \tag{17}$$

$$\varepsilon = -\chi\,\eta \tag{18}$$

The higher value of E_{HOMO} designated the electrons donor molecules while the lower value of E_{LUMO} represented the electrons acceptor molecules. The dipole moment (μ) was a considerable electronic parameter rising from the arbitrary spreading of charges on the atoms of the molecule. The adsorption of extract molecules on the metal surface and the *% IE* increased with increasing the values of E_{HOMO} and μ and decreasing the values of E_{LUMO} and ΔE (energy gap). The electronegativity (χ) of the extract gave evidence on the formation of a coordinate covalent bond between the extract and the metal that was considered an iron metal. The Pearson method was employed to estimate ΔN (the fraction of electrons transferred) between the molecule and metal surface through the following [26].

$$\Delta N = \frac{\chi_{Fe} - \chi_{ext}}{2\,(\eta_{Fe} + \eta_{ext})} \tag{19}$$

Where, χ_{Fe} stands for the electronegativity value of the iron surface planes Fe (110) = 4.82 eV which is preferred due to having higher stabilization energy and packed surface. χ_{ext} represented the electronegativity of the extract, while $\eta_{Fe} = 0$ and η_{ext} represented the hardness of iron and extract, respectively. In this study, the obtained χ_{inh} values were less than the value of electronegativity of iron (4.82 eV). Thus, we can conclude that when the metal and the extract are in contact with each other, the electrons will transfer from the Ecballium extract molecules (lower electronegativity) to the CS (higher electronegativity) till the chemical potentials become equal to form a coordinate bond. Moreover, when the values are: *0 < ΔN <3.6*, the electrons will transfer from the extract to the metal surface atom and vice versa [27]. The calculated ΔN values of the isolated compounds were more than zero and less than 3.6 suggesting that the ability of Ecballium extract molecules to give electrons to the unoccupied d-orbital of metal atoms. The global hardness (η) and its reciprocal softness (σ) parameters were very important for the activity and stability of the extract. The Ecballium extract molecules were acting as a soft base and the metal atoms as a soft acid in accordance with the HASB principle [28]. The soft molecules had a higher reactivity and a smaller energy gap than the hard ones. This facilitated transferring electrons and supported good inhibition efficiency due to the effortless adsorption done on the metallic surfaces. The back donation of charges (*ΔE back-donation = -η/4*) for the extract controlled the interaction between the Ecballium extract molecule and the metal surface [29]. When the values are: Δ*E* back-donation *<0 and η > 0*, the charge transfer will occur from the metal to the Ecballium extract molecule, followed by a back-donation from the molecule to the metal. Here, the values Δ*E* back-donation have a negative sign which means that the extract molecules preferred a back donation. The nucleophilicity index (ε) displayed the capability of a molecule to donate electrons. The higher *ε* value indicates more inhibition efficiency of the molecules. Upon these criteria, the obtained results revealed that the order of the phytochemical compounds of Ecballium extract according to their affinity to give electrons to the metal surface were VI > V > IV > III > II > I. Based on this order, we noted that the isolated compounds that had a greater number of substituents such as Oxygen atoms and hydroxyl groups (Rutin, Kaempferol-3-o-rutinoside and Cuc D) showed a larger ability to donate electrons to the metal atoms,

forming a chemical bonding during the adsorption, and consequently, they were more effective in the inhibition of CS corrosion in acidic media.
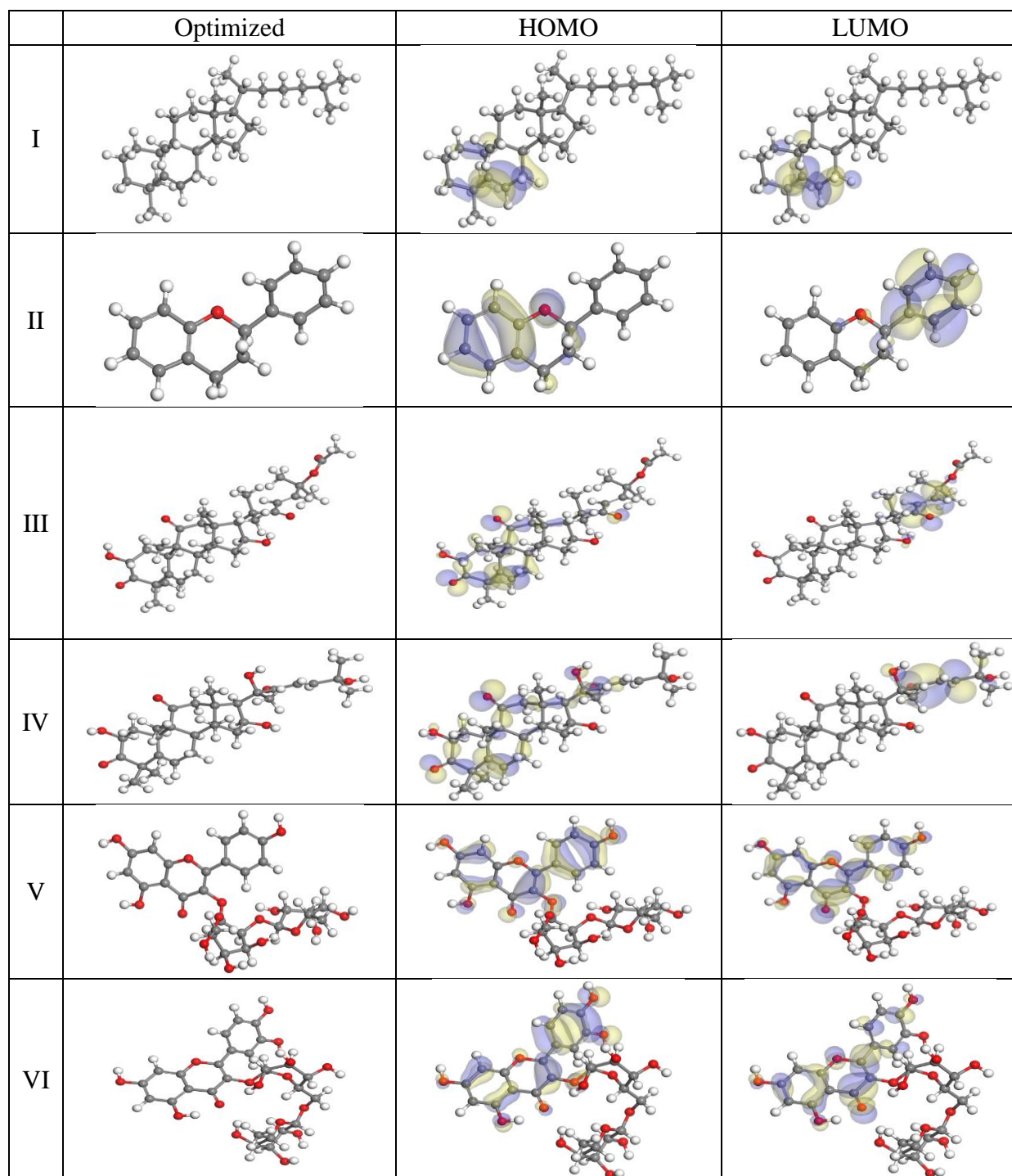
	Optimized	HOMO	LUMO
I			
II			
III			
IV			
V			
VI			

Figure 12. Optimization, HOMO and LUMO molecular structures of isolated compounds for Ecballium extract.

Table 9. The quantum chemical parameters of the isolated compounds for Ecballium extract.

Parameter	compound					
	(I)	(II)	(III)	(IV)	(V)	(VI)
E_{HOMO} (eV)	-4.854	-4.724	-4.981	-5.019	-4.799	-4.885
E_{LUMO} (eV)	0.362	-0.536	-2.136	-2.182	-2.133	-2.365
ΔE (eV)	5.216	4.188	2.845	2.837	2.666	2.520
σ (eV^{-1})	0.383	0.478	0.703	0.705	0.750	0.794
η (eV)	2.608	2.094	1.423	1.419	1.333	1.260
χ (eV)	2.246	2.630	3.559	3.601	3.446	3.625
ε (eV)	-5.858	-5.507	-5.062	-5.107	-4.594	-4.568
ΔN	0.494	0.372	0.443	0.429	0.508	0.472
$\Delta E_{back-donation}$	-0.652	-0.524	-0.356	-0.355	-0.333	-0.315
μ (Debye)	0.486	2.417	4.440	15.405	9.345	7.946

3.9 Mechanism of corrosion inhibition

The dissolution inhibition of Ecballium extract molecules may have been accredited to the presence of the electron donor groups (O) further the π-electrons in cyclic and aromatic rings in its molecular structure. The inhibitor interacted with the metal surface either through the electrostatic interaction between the inverse charge on the inhibitor molecules and the metal surface suggesting physisorption, or by sharing the nonbonding electrons to vacant d- orbital of the metal reinforcing chemisorption, or by the formation of an insoluble complex, which acted as a protective film on the surface and prevented any further dissolution of the metal [30]. The mechanism of anodic dissolution of CS in sulphate solutions was assumed by Bockris et al. [31], and the mechanism of cathodic reaction was the reduction of Hydrogen ions. The adsorption of organic extract molecules on a metal surface proceeded through the replacement of one or more adsorbed water molecules with the extract molecules in an aqueous solution as discussed before [20]. The results from the FTIR analysis indicated that the interaction between the Ecballium extract molecules and the freshly forming ferrous ions on the CS surface was accomplished by forming a complex of the following [32]:

$$Fe \leftrightarrow Fe^{2+} + 2\,e^{-} \tag{20}$$
$$Fe^{2+} + Inh_{(ads)} \leftrightarrow [Fe - Inh]_{ads}^{2+} \tag{21}$$

As for the Physisorption mechanism, the Ecballium extract molecules had several oxygen-containing heterocyclic compounds. They were easily protonated in an acid solution, producing a cationic form that reduced the evolution of hydrogen via the adsorption on the cathodic sites of CS. The adsorption of protonated inhibitor (has a positive charge) on the metal surface (has a negative charge produced from the adsorption of sulphate ions on the positive metal surface then the metal surface acquires a negative charge) was done by the electrostatic interaction between them, i.e. there might have been a synergism among SO_4^- and protonated extract [32].

$$Ecballium + xH^+ \leftrightarrow [Ecballium_x]^{x+} \tag{27}$$

While the chemisorption mechanism can be done by transferring electrons from the d-orbital of iron to the unoccupied anti-bonding orbital (π^*) of extract molecules (back bonding or retro-donation) and the reinforced adsorption.

4. CONCLUSION

The Ecballium elaterium extract anticorrosive mechanism for CS in acidic containing media was clarified both empirically and theoretically. The Ecballium elaterium extract was able to effectively inhibit the corrosion of CS in 0.5 M H_2SO_4 solution via favorable adsorption. The inhibition efficiency increased with the augment of extract concentration and temperature, yielding the maximum efficiencies of 97.5% with a concentration of 300 mg/L for the CS in the respective 0.5 M H_2SO_4 at 45°C. Also, the Ecballium elaterium extract behaved as a mixed-type corrosion inhibitor that simultaneously retarded the anodic and cathodic reactions and then reduced i_{corr} for the CS in H_2SO_4 solution. Although the charge transfer mechanism hardly changed in the presence of Ecballium elaterium extracts, it apparently increased the interfacial Rs of CS corrosion in the acidic solution. The appearance of CS was improved with the suppressed surface roughness after 24 h of the immersion in 0.5 M H_2SO_4 solution with 300 mg/L Ecballium elaterium extract at 25°C. The adsorption of the Ecballium elaterium extract on the CS in 0.5 M H_2SO_4 conformed to Temkin's isotherm model. The related kinetic and thermodynamic parameters values obtained suggested both physisorption and chemisorption mechanism at low temperature while chemisorption mechanism was favored at higher temperatures. The negative sign of $\Delta G°_{ads}$ values indicated the adsorption of the Ecballium extract molecules on the CS surface spontaneously. The quantum chemical calculations confirmed the experimental results, indicating that the Ecballium elaterium extract molecules acted as electrons donor, and the more effective isolated compounds of the extract were Rutin, Kaempferol-3-o-rutinoside and Cuc D. Based on the correlated experimental and theoretical results, the Ecballium elaterium extract can be used as an efficient corrosion inhibitor for the CS in the used acidic solution.

References

1. L.F. Li, P. Caenen, J.P. Celis, *Corros. Sci.,* 50(3) (2008)804
2. P.B. Raja, M. Ismail, S. Ghoreishiamiri, J. Mirza, M.C. Ismail, S. Kakooei, A.A. Rahim, , *Chem. Eng. Commun.,* 203(9)(2016)1145.
3. A.S. Fouda, G.E. Badr, , *Biointerface Res. Appl. Chem*., 10 (2020) 5704.
4. S. Marzorati, L. Verotta, S.P. Trasatti, *Molecules,* 24(1) (2019)1.
5. S.A. Umoren, M.M. Solomon, I.B. Obot, R.K. Suleiman, *J. Ind. Eng. Chem.,*76 (2019)91.
6. P. Parthipan, J. Narenkumar, P. Elumalai, P.S. Preethi, A. Usha Raja Nanthini, A. Agrawal, A. Rajasekar, *J. Mol. Liq.,* 240(2017)121.
7. L.T. Popoola, *Corros. Rev.*, 37 (2019) 71.
8. L. Bourebaba, B. Gilbert-López, N. Oukil, F. Bedjou, *Arab. J. Chem.*, 13 (2020) 3286.
9. H. Zarrok, A. Zarrouk, B. Hammouti, R. Salghi, C. Jama, F. Bentiss, *Corros. Sci.*, 64(2012)243.
10. L.O. Olasunkanmi, M.F. Sebona, E.E. Ebenso, *J. Mol. Struct.,* 1149 (2017)549.

11. C. Verma, L.O. Olasunkanmi, E.E. Ebenso, M.A. Quraishi, I.B. Obot, *J. Phys. Chem. C.*,120(21) (2016) 11598.
12. W.H. Li, Q. He, S.T. Zhang, C.L. Pei, B.R. Hou, *J. Appl. Electrochem.,* 38(2008)289.
13. R. Solmaz, *Corros. Sci.*, 81(2014)75.
14. E. Barsoukov, J.R. Macdonald, Fundamental of Impedance, Jhom Weily, (2005) 1-26.
15. H.M. Abd El-Lateef, *Res. Chem. Intermed.,* 42(2016)3219.
16. L.O. Olasunkanmi, I.B. Obot, E.E. Ebenso, *RSC Adv.,*90 (2016) 53933.
17. P. Singh, D.S. Chauhan, S.S. Chauhan, G. Singh, M.A. Quraishi, J. Mol. Liq., 120 (2019)11598.
18. R.W. Bosch, *Corrosion,* 57 (2001) 60.
19. M. Cui, S. Ren, H. Zhao, L. Wang, Q. Xue, *Appl. Surf. Sci*., 42(2018)3219.
20. F. El-Taib Heakal, M.A. Deyab, M.M. Osman, M.I. Nessim, A.E. Elkholy, RSC Adv., 75 (2017)47335.
21. B. Ramaganthan, M. Gopiraman, L.O. Olasunkanmi, M.M. Kabanda, S. Yesudass, I. Bahadur, A.S. Adekunle, I.B. Obot, E.E. Ebenso, *RSC Adv.,*94 *(*2015)76675.
22. E. Baran, A. Cakir, B. Yazici, *Arab. J. Chem.*, 12(8) (2019)4303.
23. S.S. Abdel-Rehim, K.F. Khaled, N.S. Abd-Elshafi, *Electrochim. Acta.,* 51(16)(2006)3269.
24. S. Chitra, K. Parameswari, A. Selvaraj, *Int. J. Electrochem. Sci.*, 5(2010) 1675.
25. S.I. Kiyooka, D. Kaneno, R. Fujiyama, *Tetrahedron Lett*., 54(4)(2013)339.
26. R.G. Pearson, *Inorg. Chem.*, 27(4) (1988)734.
27. S.K. Saha, A. Dutta, P. Ghosh, D. Sukul, P. Banerjee, *Phys. Chem. Chem. Phys.*, 18(27) (2016)17898.
28. S.K. Saha, M. Murmu, N.C. Murmu, P. Banerjee, *J. Mol. Liq., 224* (2016)629.
29. I.B. Obot, Z.M. Gasem, *Corros. Sci., 83* (2014)359.
30. E. Kamali Ardakani, E. Kowsari, A. Ehsani, *Colloids Surfaces A Physicochem. Eng. Asp.*, 586 (2020)124195.
31. J.O.M. Bockris, D. Drazic, A.R. Despic, *Electrochim. Acta.,* 4(2-4) (1961)325.
32. E.E. El-Katori, A.S. Fouda, R.R. Mohamed, *Zeitschrift Fur Phys. Chemie.,* 233(12) (2019)1713